Testing the relationship between testate amoeba community composition and environmental variables in a coastal tropical peatland

1. Graeme T. Swindles, School of Geography, University of Leeds, UK (corresponding author: g.t.swindles@leeds.ac.uk)
2. Andy J. Baird, School of Geography, University of Leeds, UK
3. Elliot Kilbride, School of Geography, University of Leeds, UK
4. Rob Low, Rigare Ltd, Abergavenny, UK
5. Omar Lopez, Panama Instituto de Investigaciones Científicas y Servicios de Alta Tecnología, Panamá & Smithsonian Tropical Research Institute, Panama

An original manuscript for *Ecological Indicators*

Keywords:

protist; testate amoebae; wetlands; hydrology; sea level; tropical rainforest

Highlights:

- We examined the ecology of testate amoebae (TA) in a tropical peatland.
- Hydrological variation is the strongest control on TA distribution.
- TA probably have limited potential as sea-level indicators in tropical wetlands.
- The new dataset was used to test an existing transfer function from Amazonia.

Abstract

We investigated the ecology of testate amoebae (TA) in a coastal tropical peatland to evaluate their potential as environmental indicators in these ecosystems. At 10 positions in five locations in a transect running into the peatland away from the coast, we measured pore-water pH, pore-water electrical conductivity, soil moisture content (MC), and water-table depth (WTD). The WTD data were collected using dipwells fitted with self-recording pressure transducers that logged at 10-minute intervals over a 25-day period. Multivariate statistical analysis showed that hydrological metrics (WTD and MC) were the strongest environmental controls on TA ($p < 0.001$) in this site, corroborating the single previous study from western Amazonia. Changes in pH and electrical conductivity, reflecting marine influence, were also significant, but less so ($p < 0.05$; $p < 0.01$ respectively). Transfer functions for WTD and MC were developed using weighted averaging partial least-squares regression, and were found to perform well under 'leave-one-out' cross validation ($R^2 = 0.80$, RMSEP = 4.64 cm; $R^2 = 0.89$; RMSEP = 1.57 cm). Our results clarify the autecology of several taxa found in tropical peatlands. *Centropyxis aculeata* is an unambiguous indicator of surface water, *Hyalosphenia subflava* "minor" (<60 μm length) is a dry indicator, whereas *Hyalosphenia subflava* "major" (>60 μm length) lives in wetter conditions. The difference in habitat preference of the two forms of *Hyalosphenia subflava* suggests that this taxon is most probably a species complex. We use the new high-quality dataset to test an existing transfer function from western Amazonia: the results show that the previous model has good predictive power for reconstructing past WTDs in tropical peatlands ($r = 0.87$; $p < 0.005$). The reconstruction of sea-level change from tropical coastal wetlands may prove problematic because the key indicators of marine influence, reflected in pH and electrical conductivity, are taxa with weak idiosomic tests that do not preserve readily in the peat archive (e.g. *Tracheleuglypha dentata*, *Trinema lineare*). Our work shows the potential of using high-quality hydrological measurements for increasing the precision of transfer function models.

1. Introduction

Tropical peatlands represent a globally-important carbon store and can be found in Asia, Central and South America, and Africa (Page et al., 2011; Dargie et al., 2017). They have been severely damaged in Southeast Asia through drainage and subsequent conversion to palm oil and wood pulp production (Posa et al., 2011; Green and Page, 2017). This has led to extensive fires with significant implications for air quality and human health (Page and Baird, 2016). Coastal tropical peatlands have also been identified as particularly vulnerable to sea-level rise, with ~61,000 km^2 of them lying ≤ 5 m above sea-level (Whittle and Gallego-Sala, 2016). However, relatively little is known about how tropical peatlands have developed through time, and their ecohydrological responses to climate change and sea-level rise remain unclear (Swindles et al., 2018).

Multiproxy palaeoenvironmental studies of tropical peatlands are in their infancy (e.g. Hapsari et al., 2017; Swindles et al., 2018), and much uncertainty remains over the efficacy of proxy-based reconstruction methods in these systems. Testate amoebae (TA) are dominant microbial consumers in peatlands, representing up to 30% of the total microbial biomass, and may have a major influence on the ecological functioning of peatland ecosystems through nutrient and carbon cycling (Gilbert et al., 1998; Mitchell et al., 2003). TA are sensitive wetness indicators (e.g. Charman and Warner, 1992; Swindles et al., 2009; Turner et al., 2013; Amesbury et al., 2016), and have become a standard tool for palaeohydrological reconstruction in northern peatlands using statistical ‘transfer functions’ (e.g. Woodland et al., 1998; Booth et al., 2008; Swindles et al., 2015). To date, TA have only been used as hydrological indicators in one tropical peatland: Aucayacu, a raised peat dome in Peruvian Amazonia (Reczuga et al., 2015; Swindles et al., 2014, 2016, 2018). This work has shown that the distribution of TA is controlled primarily by hydrological variables, mirroring findings from northern ombrotrophic peatlands (Swindles et al., 2014). It has also been shown that a transfer function can be used to infer major hydrological changes down-core, although problems with low test concentration and preservation limit the sensitivity of the reconstruction (Swindles et al., 2016, 2018).

Here we present the first investigation of peatland testate amoebae communities from Central America. Specifically, we (i) investigate the ecology of TA in a Panamanian coastal peatland; (ii) use high-quality automatically-logged water-table depth (WTD) determinations to test the hypothesis that hydrological variables are the strongest environmental control on the distribution of TA; (iii) use the data to test the existing TA transfer function from Peruvian Amazonia; (iv) evaluate the potential of TA as sea-level indicators.

2. Study site

Oropel Swamp (Baird et al., 2017) (Fig. 1) is a coastal tropical peatland in Bocas del Toro province, northwest Panama, and represents part of the wider Changuinola peat swamp complex (Phillips et al., 1997). Coring has revealed peat up to 6.5 m thick across the site (Fig. 2). The climate of this region is humid-tropical with no distinct dry season; average annual temperature is c. 26°C and average annual precipitation is around 3200 mm (Phillips et al., 1997; Baird et al., 2017).

3. Method

3.1 Fieldwork

We established a NE-SW transect encompassing all vegetation zones across the site from 9.383460°N, 82.366030°W to 9.379308°N, 82.367403°W (Figs 1 and 3). The transect was surveyed to an arbitrary datum using a Leica NA720 automatic optical level and staff, and the locations of five sampling 'stations', were recorded using a portable GPS (Fig. 1). All elevations here are reported as ‘above arbitrary datum’ (AAD) which was set 3 m below the survey point furthest from the shore (Fig. 2). Major changes in vegetation composition were recorded along the transect and, in each major type, a sampling station was established. Water tables at each station were measured using two dipwells fitted with self-recording pressure transducers. At the stations containing wells 5,6, 7 and 8, one well was placed in a ridge (dipwells 5 and 7) and one in a hollow or pool (dipwells 6 and 8). The dipwells comprised 0.032 m diameter auger holes excavated to a depth of 0.5-0.85 m (depending on location) below the ground surface. The holes were fitted with high density polyethylene tubing with an outside diameter of 0.032 m and an inside diameter of 0.025 m. The tubing was perforated with 0.3-mm wide, 30-mm long horizontal slots, placed 5-mm apart in two lines running vertically down the tube (1 m length), and was supplied by van Walt UK Ltd. All of the wells showed very rapid response times; the times taken for water-level equilibration after a slug of water was removed from the wells ranged from a few seconds to a few minutes (always less than five minutes). Water levels in the dipwells were measured using vented Level TROLL 500 self-logging pressure transducers (InSitu Inc., Fort Collins, accuracy: 0.0035 m or better, resolution: 0.00035 m). Each pressure transducer was independently calibrated, and the resulting calibration equation used to convert instrument output to water levels. The pressure transducers were in place between 2nd and 27th November 2014 and logged at 10-minute intervals. From these data, we calculated the mean, maximum, and minimum WTDs below the ground surface. This represents one of the most detailed water-table datasets collected from a tropical peatland. During the same period, a total of 194.8 mm fell (recorded on-site using an automatic weather station), which represents approximately 6% of typical annual rainfall at the site (estimated at 3175 mm – Baird et al., 2017); i.e., average daily rainfall during the monitoring period was similar to that for a typical year as a whole. As well as being neither particularly dry nor wet, the monitoring period contained runs of dry days interspersed with wetter spells, again 'capturing' what is usual for the area (Paton, 2015 Baird et al., 2017;). Average air temperature at the site during the monitoring period was 25.2 °C.

Four litter samples of approximately 5 cm^3 each were taken from around each dipwell and placed into Ziplok™ bags for analysis of TA. The pH and electrical conductivity of the water just below the water table was measured by syringing *c*. 30 mL water from the dipwells into a beaker into which measurement probes were inserted. Conductivity was measured using a Horiba (Horiba Ltd, Kyoto, Japan) Twin Cond B-173 meter (repeatability: ± 1%), while pH was measured using a Horiba LAQUAtwin B-712 meter (accuracy: ± 0.1 pH unit).

3.2 Laboratory analysis

Litter samples were returned to the laboratory at the University of Leeds and stored at 4ºC prior to analysis. One half of the litter sample was used to determine soil moisture content (MC) and loss-on-ignition (organic content) using standard laboratory methods (105°C for 24 hours; 550°C for 4 hours; Chambers et al., 2011). TA were extracted from the peat samples through sieving at 300 μm and back-sieving at 15 μm following Booth et al. (2010). TA were counted under transmitted light at 200-400× magnification and were identified using morphology, composition, size and colour to distinguish taxa. At least 200 specimens were counted in each sample to ensure statistical reliability (e.g. Patterson and Fishbein, 1989). TA were identified using several sources (Charman et al., 2000; Ogden and Hedley, 1980; Mazei et al., 2006; Meisterfeld, 2000ab; Siemensma, 2017). The taxonomy used a morphospecies approach in certain circumstances, where a designation that includes other species or several morphotypes is referred to as a "type". Minor taxa with a maximum abundance < 2% were removed prior to statistical analysis.

3.3 Statistical analysis

The Shannon Diversity Index (SDI) was calculated for each sample to examine faunal diversity in addition to species richness. Nonmetric Multidimensional Scaling (NMDS) was used to examine the relationship between TA community composition and environmental variables. Bray-Curtis dissimilarity was used and the optimal solution was identified through comparison of final stress values following each run. Environmental variables were fitted to the solution post hoc using the 'envfit' procedure with 999 permutations. The analysis was carried out using the 'vegan' package (Oksanen et al., 2012) in R v. 3.3.2 (R Core Team, 2016).

Transfer functions were constructed using weighted averaging (WA), tolerance-downweighted weighted averaging (WA-Tol), weighted averaging partial least-squares (WA-PLS), and maximum likelihood (ML) regression models using the C2 software package (Juggins, 2007). The performance of the transfer function models was evaluated using R^2 and the root mean square error of prediction (RMSEP) with leave-one-out (LOO) cross validation (jack-knifing). An existing TA-based transfer function from a peatland in Amazonia (Swindles et al., 2014) was used to predict WTDs for the Oropel Swamp contemporary samples, and sample-specific errors of prediction were calculated from 999 bootstrap cycles. Tolerance and optima statistics were also calculated for each taxon through weighted averaging regression.

4. Results

4.1 Site characteristics

Oropel Swamp has a distinct vegetation zonation comprising five main types: (i) central *Cladium*-dominated plain; (ii) stunted *Campnosperma panamensis* forest with (*Cladium*) sawgrass; (iii) *Campnosperma panamensis* – *Symphonia globulifera* hardwood forest; (iv) mixed *Campnosperma panamensis* – *Euterpe precatoria* – *Raphia taedigera* forest; and (v) brackish mangrove edge with *Cassipourea elliptica* and *Chrysobalanus icaco* scrub (Table 1, Fig. 3).

Further information about the plant assemblages in the site is provided in Supplementary file 1. There are major variations in microtopography across the peatland with distinct microforms including ridges, tree-root hummocks, hollows and pools. Water pH and electrical conductivity values in all but the brackish margin of the peatland suggest that it functions as an ombrotrophic system, despite lying < 1 m above sea-level (Table 1; Figs 2 and 3). A series of ridges in the site appear to prevent sea-water ingress via surface flow.

4.2 Ecology of testate amoebae

A total of 41 TA taxa from 19 genera were identified in Oropel Swamp (Figs 3 and 4, Table 2). The most common taxa include *Centropyxis aculeata*, *Euglypha rotunda* type, *Hyalosphenia subflava*, *Phryganella acropodia* and *Trinema lineare*. Two forms of *Hyalosphenia subflava* were encountered – “major” (>60 μm length) and “minor” (<60 μm length). The taxon *Hyalosphenia subflava* appears to have a bimodal size distribution in tropical peatlands which is interpreted here as two distinct forms (also see Swindles et al., 2014). *Centropyxis aculeata, Cyphoderia* sp. 1, *Hyalosphenia subflava* “major” and *Lesquereusia spiralis* are indicators of wet surface conditions in the peatland. Taxa with siliceous idiosomic tests (e.g. *Tracheleuglypha dentata*, *Trinema lineare*) were abundant in the samples adjacent to the coast. SDI values of the samples range between 1.5 and 2.7. SDI and species richness are lowest towards the coast, suggesting a stressed community in this location owing to raised surface and pore-water salinity (Fig. 3). A strong influence of hydrological variables on the distribution of TA is suggested by the NMDS analysis and envfit (Fig. 4), although the other variables are still significant: MC ($R^2 = 0.81$; $p < 0.0001$), WTD ($R^2 = 0.67$; $p < 0.0001$), electrical conductivity ($R^2 = 0.26$; $p < 0.01$), pH ($R^2 = 0.24$; $p < 0.05$). When the samples from the two dipwells affected by marine influence are removed, the results are as follows: MC ($R^2 = 0.81$; $p < 0.0001$), WTD ($R^2 = 0.69$; $p < 0.0001$), Conductivity ($R^2 = 0.19$; $p < 0.05$), pH ($R^2 = 0.15$; $p = 0.114$).

The performance statistics for the transfer function models are shown in Table 3. The best performing models for WTD and MC are based on weighted averaging partial least-squares regression (WAPLS). Component 3 was selected in both cases to ensure good performance, but avoiding a statistical 'over-fit' (Fig. 6). The performance statistics of the WTD and MC transfer function are as follows: WTD – R^2_{apparent} = 0.90; $\mathrm{RMSE}_{\mathrm{apparent}}$ = 3.29 cm; R^2_{LOO} = 0.80; $\mathrm{RMSE}_{\mathrm{LOO}}$= 4.64 cm; MC – R^2_{apparent} = 0.94; $\mathrm{RMSE}_{\mathrm{apparent}}$ = 1.14 %; R^2_{LOO} = 0.89; $\mathrm{RMSE}_{\mathrm{LOO}}$= 1.57 %. Tolerance and optima statistics illustrate the variations in the ecology of the taxa in relation to WTD and MC (Fig. 7). No sample screening or removal was needed owing to excellent transfer function performance using the complete dataset. This contrasts with most other transfer functions that have required some samples to be removed to improve model performance (e.g. Swindles et al., 2009, 2014).

4.3 Testing the Amazonian transfer function

The transfer function of Swindles et al. (2014) from western Amazonia was tested using the new dataset from Oropel Swamp. A WAPLS component 3 model was applied to the TA data presented here. A strong relationship was found between the predicted and observed WTDs (r = 0.87; p < 0.005) suggesting that the Amazonian model has good predictive power for reconstructing past WTDs in tropical peatlands (Fig. 8). However, the fit between modelled and observed departed from the 1:1 line and this is discussed below.

5. Discussion

Our study confirms the value of TA as environmental indicators in tropical peatlands. In particular, our results highlight the sensitivity of TA in a tropical context to hydrological variation and are similar to those from studies of mid- and high-latitude peatlands (e.g. Booth, 2008; Swindles et al., 2016; Amesbury et al., 2016). There is large similarity between the ecology of the TA taxa here and what was found previously in the western Amazonian peatland (Swindles et al., 2014). Notable minor differences between the TA communities in these studies include the lower abundances of *Cryptodifflugia oviformis* and lack of *Argynnia spicata* (suggested to be biogeographically limited to the Southern Hemisphere) in Oropel Swamp. Our work reinforces the ecological preferences of a number of key indicator taxa (e.g. *Centropyxis aculeata* as an unambiguous wet indicator) and that *Hyalosphenia subflava* "minor" and "major" have different hydrological preferences (Fig. 7). Given the range of habitats, it is likely that *Hyalosphenia subflava* is a species complex, although this needs to be investigated further through genetic analysis (e.g. Heger et al., 2013; Oliverio et al., 2014; Roland et al., 2017).

The transfer function from Oropel Swamp has excellent performance statistics, which may suggest that the precision of transfer functions can be improved through high-quality auto-logged WTD determinations. One of the potential concerns with previous studies (including the one in western Amazonia) is that they have used a 'one-off' WTD measurement from the TA sample extraction point (see Woodland et al., 1998; Booth, 2008; Swindles et al., 2015), whereas here we used WTD averages based on more than 3500 readings. However, the finding that the previous model from western Amazonia has good predictive power for reconstructing modern WTD in Oropel Swamp suggests that the 'one-off' WTD measurements are, at least to some degree, sufficient to drive a hydrological gradient for TA transfer-function development. Nevertheless, the western Amazonian transfer function somewhat under-predicts WTD at the dry hydrological extreme and under-predicts surface water depth at the wet hydrological extreme, which may, in part, be caused by (i) the decoupling of TA from very deep water tables and (ii) the lack of ability of TA to discriminate variations in surface water depth (e.g. Swindles et al., 2009; Swindles et al., 2015). However, it is notable that the Oropel Swamp transfer function does pick up these extremes well.

There has been widespread use of TA for reconstructing Late Holocene sea-level change from coastal marshes (Gehrels et al., 2001; Barnett et al., 2017). However, this approach has not yet been evaluated in tropical environments. We suggest that TA have limited potential as sea-level indicators in tropical wetlands because the key indicators of brackish conditions comprise taxa with weak idiosomic tests that do not preserve readily in the peat archive (e.g. *Tracheleuglypha dentata*, *Trinema lineare*). Furthermore, hydrological variables are stronger environmental controls on the distribution of TA in Oropel Swamp than the variables related to marine influence (pH and electrical conductivity). Analysis of TA communities in other coastal tropical wetlands is needed to test this provisional finding.

Tropical peatlands are globally-important ecosystems and carbon stores that are under threat from human impacts and climate change (Page et al., 2011; Page and Baird, 2016). However, much remains unknown about the microbial ecology of these ecosystems (e.g. Swindles et al., 2014; Reczuga et al., 2015). Our study shows that TA are unambiguous hydrological indicators in tropical peatlands and that transfer functions have good predictive power. The next stage of this research is to examine subfossil TA from Oropel Swamp and apply the transfer functions presented here to reconstruct the palaeohydrological dynamics of the peatland (e.g. Swindles et al., 2016). Our work represents the first study of peatland TA in Central America and in a coastal tropical peatland. We recommend future studies compare TA communities from tropical peatlands in Central and South America, Africa and SE Asia to examine wide-scale variations in biogeography and TA autecology.

6. Conclusions

1. We investigated the ecology of testate amoebae (TA) and their efficacy as hydrological and sea-level indicators in a coastal tropical peatland.

2. Our results clarify the autecology of several taxa found in tropical peatlands. *Centropyxis aculeata* is an unambiguous indicator of surface water; *Hyalosphenia subflava* “minor” (<60 μm) is a dry indicator; *Hyalosphenia subflava* “major” (>60 μm) lives in wetter conditions than the “minor” form of this taxon.
3. Hydrological variation is the strongest control on TA distribution in the tropical peatland, corroborating a study from western Amazonia and previous work on high and mid-latitude peatlands.
4. TA have limited potential as sea-level indicators in tropical wetlands because the key indicators are composed of weak siliceous idiosomic tests with poor preservation potential.
5. We use the new TA dataset alongside high-quality hydrological determinations and other environmental data to i) develop a new transfer function for hydrological reconstruction; and ii) test an existing transfer function from western Amazonia. The performance of the transfer function was excellent and no sample screening to improve model performance was needed. Our results showed the existing transfer function from western Amazonia had good predictive power.

References

Amesbury, M.J., Swindles, G.T., Bobrov, A., Charman, D.J., Holden, J., Lamentowicz, M., Mallon, G., Mazei, Y., Mitchell, E.A.D., Payne, R.J., Roland, T.P., Turner, T.E., Warner, B.G., 2016. Development of a new pan-European testate amoeba transfer function for reconstructing peatland palaeohydrology. Quat. Sci. Rev. 152, 132–151. doi:10.1016/j.quascirev.2016.09.024

Baird, A.J., Low, R., Young, D., Swindles, G.T., Lopez, O.R., Page, S., 2017. High permeability explains the vulnerability of the carbon store in drained tropical peatlands. Geophys. Res. Lett. 44, 1333–1339. doi:10.1002/2016GL072245

Barnett, R.L., Newton, T.L., Charman, D.J., Gehrels, W.R., 2017. Salt-marsh testate amoebae as precise and widespread indicators of sea-level change. Earth-Science Rev. 164, 193–207. doi:10.1016/J.EARSCIREV.2016.11.002

Booth, R.K., Lamentowicz, M., Charman, D.J., 2010. Preparation and analysis of testate amoebae in peatland palaeoenvironmental studies. Mires Peat 7, 1–7.

Booth, R.K., 2008. Testate amoebae as proxies for mean annual water-table depth in *Sphagnum*-dominated peatlands of North America. J. Quat. Sci. 23, 43–57. doi:10.1002/jqs.1114

Chambers, F.M., Beilman, D.W., Yu, Z., 2011. Methods for determining peat humification and for quantifying peat bulk density, organic matter and carbon content for palaeostudies of climate and peatland carbon dynamics. Mires Peat 7, 1–10.

Charman, D.J., Hendon, D., Woodland, W.A., 2000. The Identification of Testate Amoebae (Protozoa: Rhizopoda) in Peats. Quaternary Research Association. Technical Guide No. 9. 147 pp.

Charman, D.J., Warner, B.G., 1992. Relationship between testate amoebae (Protozoa: Rhizopoda) and microenvironmental parameters on a forested peatland in northeastern Ontario. Can. J. Zool. 70, 2474–2482. doi:10.1139/z92-331

Dargie, G.C., Lewis, S.L., Lawson, I.T, Mitchard, E.T.A., Page, S.E., Bocko, Y.E., Ifo, S.A., 2017. Age, extent and carbon storage of the central Congo Basin peatland complex. Nature 542, 86–90. doi:10.1038/nature21048

Gehrels, W.R., Roe, H.M., Charman, D.J., 2001. Foraminifera, testate amoebae and diatoms as sea-level indicators in UK saltmarshes: a quantitative multiproxy approach. J. Quat. Sci. 16, 201–220. doi:10.1002/jqs.588

Gilbert, D., Amblard, C., Bourdier, G., Francez, A.-J., 1998. The microbial loop at the surface of a peatland: structure, function, and impact of nutrient input. Microb. Ecol. 35, 83–93. doi:10.1007/s002489900062

Google Earth 6.0., 2008. Oropel Swamp. 9°22'53.9"N 82°21'58.6"W, viewed 31 August 2016. http://www.google.com/earth/index.html.

Green, S.M., Page, S., 2017. Tropical peatlands: current plight and the need for responsible management. Geol. Today 33, 174–179. doi:10.1111/gto.12197

Hapsari, K.A., Biagioni, S., Jennerjahn, T.C., Reimer, P.M., Saad, A., Achnopha, Y., Sabiham, S., Behling, H., 2017. Environmental dynamics and carbon accumulation rate of a tropical peatland in Central Sumatra, Indonesia. Quat. Sci. Rev. 169, 173–187. doi:10.1016/j.quascirev.2017.05.026

Heger, T.J., Mitchell, E.A.D., Leander, B.S., 2013. Holarctic phylogeography of the testate amoeba *Hyalosphenia papilio* (Amoebozoa: Arcellinida) reveals extensive genetic diversity explained more by environment than dispersal limitation. Mol. Ecol. 22, 5172–5184. doi:10.1111/mec.12449

Juggins. S., 2007. C2 Version 1.5 User guide. Software for ecological and palaeoecological data analysis and visualisation. Newcastle University, Newcastle upon Tyne, UK. 73 pp.

Mazei, Y.A., Tsyganov, A., 2006. Freshwater testate amoebae. KMK, Moscow. 304 pp.

Meisterfeld, R., 2000a. Arcellinida, in: Lee, J., Leedale, G., Bradbury, P. (Eds.), The Illustrated Guide to the Protozoa. Vol. 2, Society of Protozoologists, Lawrence, Kansas, pp. 1054–1084.

Meisterfeld, R., 2000b. Testate amoebae with filopodia, in: Lee, J.J., Leedale, G.F., Bradbury, P. (Eds.), The Illustrated Guide to the Protozoa. Vol. 2, Society of Protozoologists, Lawrence, Kansas, pp. 1054–1084.

Mitchell, E.A.D., Gilbert, D., Buttler, A., Amblard, C., Grosvernier, P., Gobat, J.-M., 2003. Structure of microbial communities in *Sphagnum* peatlands and effect of atmospheric carbon dioxide enrichment. Microb. Ecol. 46, 187–199. doi:10.1007/BF03036882

Ogden, C.G., Hedley, R.H., 1980. An atlas of freshwater testate amoebae. Oxford University Press [for the] British Museum (Natural History). 228 pp.

Oksanen, J.G.B., F. Kindt, R. Legendre, P. Minchin, P.R. O'Hara, R.B. Simpson, G.L. Solymos, P. Stevens, H.H. Wagner, H.H., 2012. vegan: Community Ecology Package. R package version 2.0-5. http://CRAN.R-project.org/package=vegan

Oliverio, A.M., Lahr, D.J.G., Nguyen, T., Katz, L.A., 2014. Cryptic diversity within morphospecies of testate amoebae (Amoebozoa: Arcellinida) in New England bogs and fens. Protist 165, 196–207. doi:10.1016/j.protis.2014.02.001

Page, S.E., Baird, A.J., 2016. Peatlands and global change: response and resilience. Annu. Rev. Environ. Resour. 41, 35–57. doi:10.1146/annurev-environ-110615-085520

Page, S.E., Rieley, J.O., Banks, C.J., 2011. Global and regional importance of the tropical peatland carbon pool. Glob. Chang. Biol. 17, 798–818. doi:10.1111/j.1365-2486.2010.02279.x

Paton, S. 2015. Meteorological and Oceanographic Summary for the Bocas del Toro Research Station. Smithsonian Tropical Research Institute, Panamá City, Panamá, 34 pp.

Patterson, R.T., Fishbein, E., 1989. Re-examination of the statistical methods used to determine the number of point counts needed for micropaleontological quantitative research. J. Paleontol. 63, 245–248. doi:10.1017/S0022336000019272

Phillips, S., Rouse, G.E., Bustin, R.M., 1997. Vegetation zones and diagnostic pollen profiles of a coastal peat swamp, Bocas del Toro, Panamá. Palaeogeogr. Palaeoclimatol. Palaeoecol. 128, 301–338. doi:10.1016/S0031-0182(97)81129-7

Posa, M.R.C., Wijedasa, L.S., Corlett, R.T., 2011. Biodiversity and conservation of tropical peat swamp forests. BioScience 61, 49–57. doi:10.1525/bio.2011.61.1.10

R Core Team, 2016. R: A language and environment for statistical computing. R Foundation for Statistical Computing, Vienna, Austria. URL https://www.R-project.org/

Reczuga, M.K., Swindles, G.T., Grewling, Ł., Lamentowicz, M., 2015. Arcella peruviana sp. nov. (Amoebozoa: Arcellinida, Arcellidae), a new species from a tropical peatland in Amazonia. Eur. J. Protistol. 51, 437–449. doi:10.1016/j.ejop.2015.01.002

Roland, T.P., Amesbury, M.J., Wilkinson, D.M., Charman, D.J., Convey, P., Hodgson, D.A., Royles, J., Clauß, S., and Völcker, E., 2017. Taxonomic implications of morphological complexity within the testate amoeba genus *Corythion* from the Antarctic Peninsula: Protist 168, 565–585. https://doi.org/10.1016/j.protis.2017.07.006

Siemensma, F.J., 2017. Microworld, world of amoeboid organisms. World-wide electronic publication, Kortenhoef, the Netherlands. https://www.arcella.nl

Swindles, G.T., Charman, D.J., Roe, H.M., Sansum, P.A., 2009. Environmental controls on peatland testate amoebae (Protozoa: Rhizopoda) in the North of Ireland: Implications for Holocene palaeoclimate studies. J. Paleolimnol. 42, 123–140. doi:10.1007/s10933-008-9266-7

Swindles, G.T., Reczuga, M., Lamentowicz, M., Raby, C.L., Turner, T.E., Charman, D.J., Gallego-Sala, A., Valderrama, E., Williams, C., Draper, F., Honorio Coronado, E.N., Roucoux, K.H., Baker, T., Mullan, D.J., 2014. Ecology of testate amoebae in an Amazonian peatland and development of a transfer function for palaeohydrological reconstruction. Microb. Ecol. 68. 284–98 doi:10.1007/s00248-014-0378-5

Swindles, G.T., Amesbury, M.J., Turner, T.E., Carrivick, J.L., Woulds, C., Raby, C., Mullan, D., Roland, T.P., Galloway, J.M., Parry, L., Kokfelt, U., Garneau, M., Charman, D.J., Holden, J.,. Evaluating the use of testate amoebae for palaeohydrological reconstruction in permafrost peatlands. Palaeogeogr. Palaeoclimatol. Palaeoecol. 424, 111–122. doi:10.1016/j.palaeo.2015.02.004

Swindles, G.T., Holden, J., Raby, C.L., Turner, T.E., Blundell, A., Charman, D.J., Menberu, M.W., Kløve, B., 2015b. Testing peatland water-table depth transfer functions using high-resolution hydrological monitoring data. Quat. Sci. Rev. 120, 107–117. doi:10.1016/j.quascirev.2015.04.019

Swindles, G.T., Lamentowicz, M., Reczuga, M., Galloway, J.M., 2016. Palaeoecology of testate amoebae in a tropical peatland. Eur. J. Protistol. 55, 181–189. doi:10.1016/j.ejop.2015.10.002

Swindles, G.T., Morris, P.J., Whitney, B., Galloway, J.M., Gałka, M., Gallego-Sala, A., Macumber, A.L., Mullan, D., Smith, M.W., Amesbury, M.J., Roland, T.P., Sanei, H., Patterson, R.T., Sanderson, N., Parry, L., Charman, D.J., Lopez, O., Valderamma, E., Watson, E.J., Ivanovic, R.F., Valdes, P.J., Turner, T.E., Lähteenoja, O., 2018. Ecosystem state shifts during long-term development of an Amazonian peatland. Glob. Chang. Biol. 42, 738–757. doi:10.1111/gcb.13950

Turner, T.E., Swindles, G.T., Charman, D.J., Blundell, A., 2013. Comparing regional and supra-regional transfer functions for palaeohydrological reconstruction from Holocene peatlands. Palaeogeogr. Palaeoclimatol. Palaeoecol. 369, 395–408. doi:10.1016/J.PALAEO.2012.11.005

Whittle, A., Gallego-Sala, A. V., 2016. Vulnerability of the peatland carbon sink to sea-level rise. Sci. Rep. 6, 28758. doi:10.1038/srep28758

Woodland, W.A., Charman, D.J., Sims, P.C., 1998. Quantitative estimates of water tables and soil moisture in Holocene peatlands from testate amoebae. The Holocene 8, 261–273. doi:10.1191/095968398667004497

Figure captions

Fig 1. The sampling locations (dipwells 1-10) and topographic survey line in Oropel Swamp (Google Earth, 2016).

Fig 2. Topographic and stratigraphic survey data from Oropel Swamp, showing the location of the points from which cores were extracted. Dipwells 1 and 2 were located at core point 1, Dipwells 3 and 4 were at core point 2, Dipwells 5 and 6 were at core point 3, Dipwells 7 and 8 were at core point 4, and Dipwells 9 and 10 at core point 1. The mean high sea water level (MHW) level during the monitoring period is also illustrated.

Fig 3. Environmental variables, key indicator TA and diversity information plotted with distance from the shore (four TA samples were analysed from each of the ten dipwells). Main vegetation zones are illustrated: BP = bog plain, SF = stunted forest; HFR = hardwood forest ridge; HFP = hardwood forest pool; MFR = mixed forest ridge; MFP = mixed forest pool; BS = brackish shrub.

DW = dipwell. The electrical conductivity values at DW10 are in percentage salinity units (based on mass). Electrical conductivity is plotted on a logarithmic scale. The mean high sea water (MHW) level during the monitoring period is illustrated.

Fig 4. Percentage TA data from Oropel Swamp plotted with distance from the shore. Main vegetation zones are illustrated: BP = bog plain, SF = stunted forest; HFR = hardwood forest ridge; HFP = hardwood forest pool; MFR = mixed forest ridge; MFP = mixed forest pool; BS = brackish shrub. DW = dipwell.

Fig 5. NMDS ordination of TA data from Oropel Swamp (Bray-Curtis distance). Environmental variables fitted using the 'envfit' procedure are shown. Refer to Table 2 for full taxon names and sample codes. Environmental variables include water-table depth (WTD), soil moisture content (MC), electrical conductivity (COND) and pH. Panel (a) is an NMDS ordination of the complete dataset; (b) has samples from coastal Dipwells 9 and 10 removed. Blue boxes highlight the coastal samples and yellow boxes represent the dry peat ridges. Purple boxes represent the samples from generally wet conditions in the peatland.

Fig. 6. Graph of WAPLS model-estimated versus observed (a) WTD (cm); and (b) MC (%). 1:1 lines are shown and represent a hypothetical perfect fit between observed and model-estimated values.

Fig. 7. Tolerance-optima statistics of key taxa from the WAPLS transfer function model. *Hyalosphenia subflava* "major" and "minor" are highlighted in red.

Fig. 8. Plot showing predictions of WTD based on a transfer function from western Amazonia (Swindles et al., 2014) against observed WTDs from Oropel Swamp. A linear regression between the variables is also shown. The *y*-axis error bars are derived from 999 bootstrap cycles; whereas *x*-axis error bars represent the maximum and minimum recorded WTDs.

Table 1. Site characteristics.

Table 2. Taxon names, authorities and codes.

Table 3. Transfer function performance statistics.

Supplementary file 1. Vegetation zones of Oropel Swamp.

Figure 1
Click here to download high resolution image

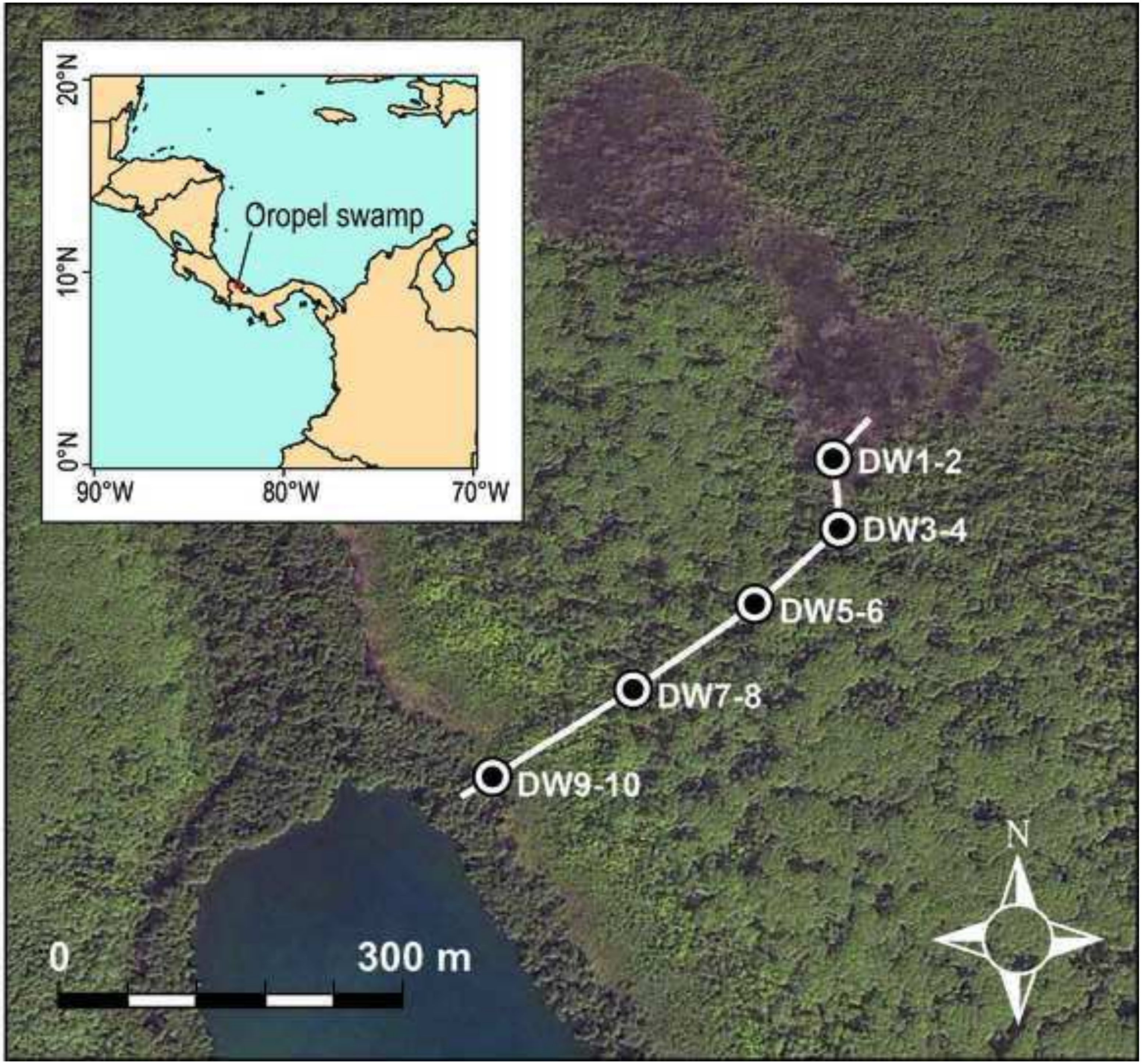

Figure 2

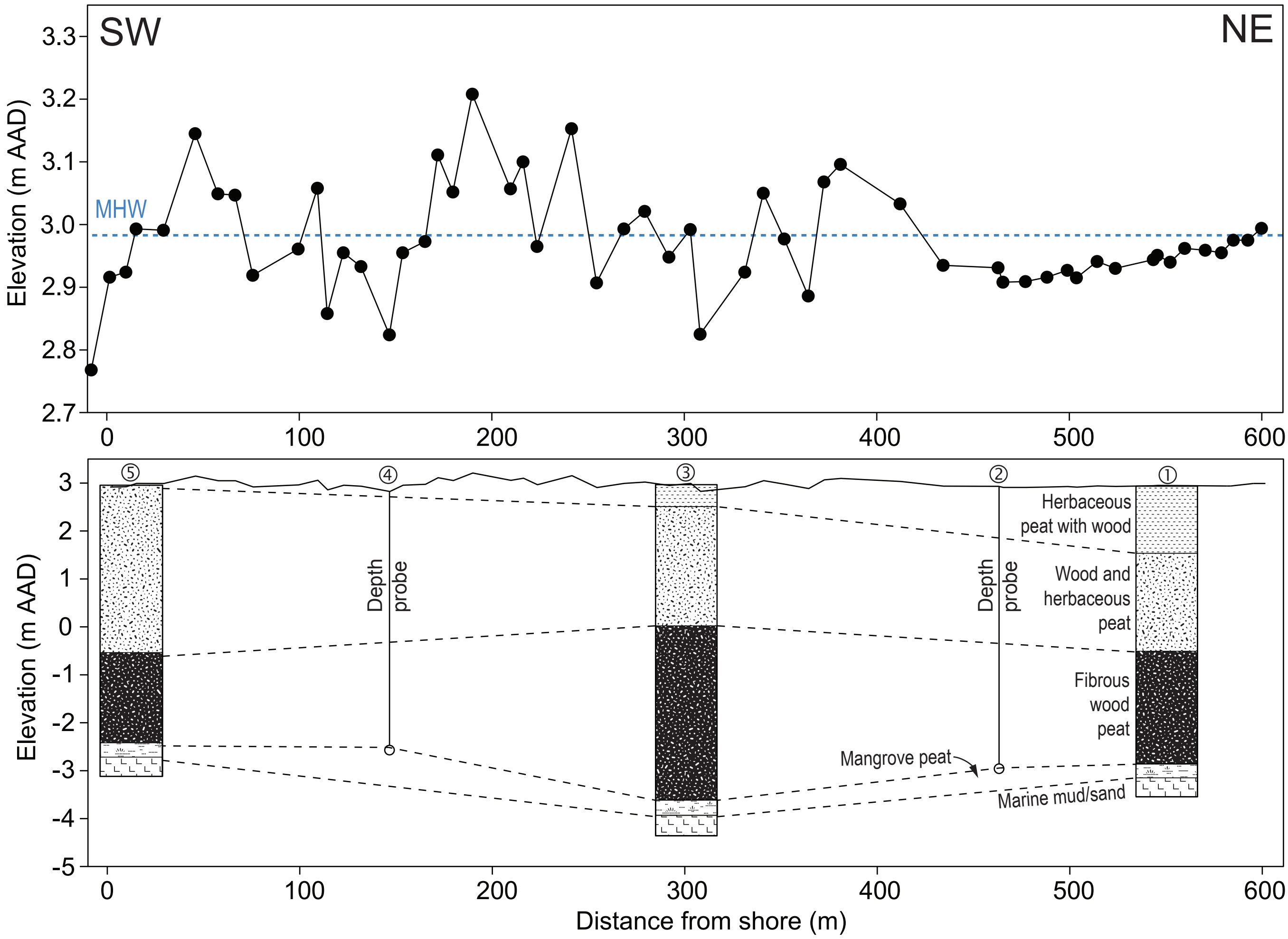

SW
NE
MHW
Elevation (m AAD)
3.3
3.2
3.1
3.0
2.9
2.8
2.7
0
100
200
300
400
500
600
⑤
④
③
②
①
Herbaceous peat with wood
Wood and herbaceous peat
Fibrous wood peat
Depth probe
Depth probe
Mangrove peat
Marine mud/sand
Elevation (m AAD)
3
2
1
0
-1
-2
-3
-4
-5
0
100
200
300
400
500
600
Distance from shore (m)

Figure 3

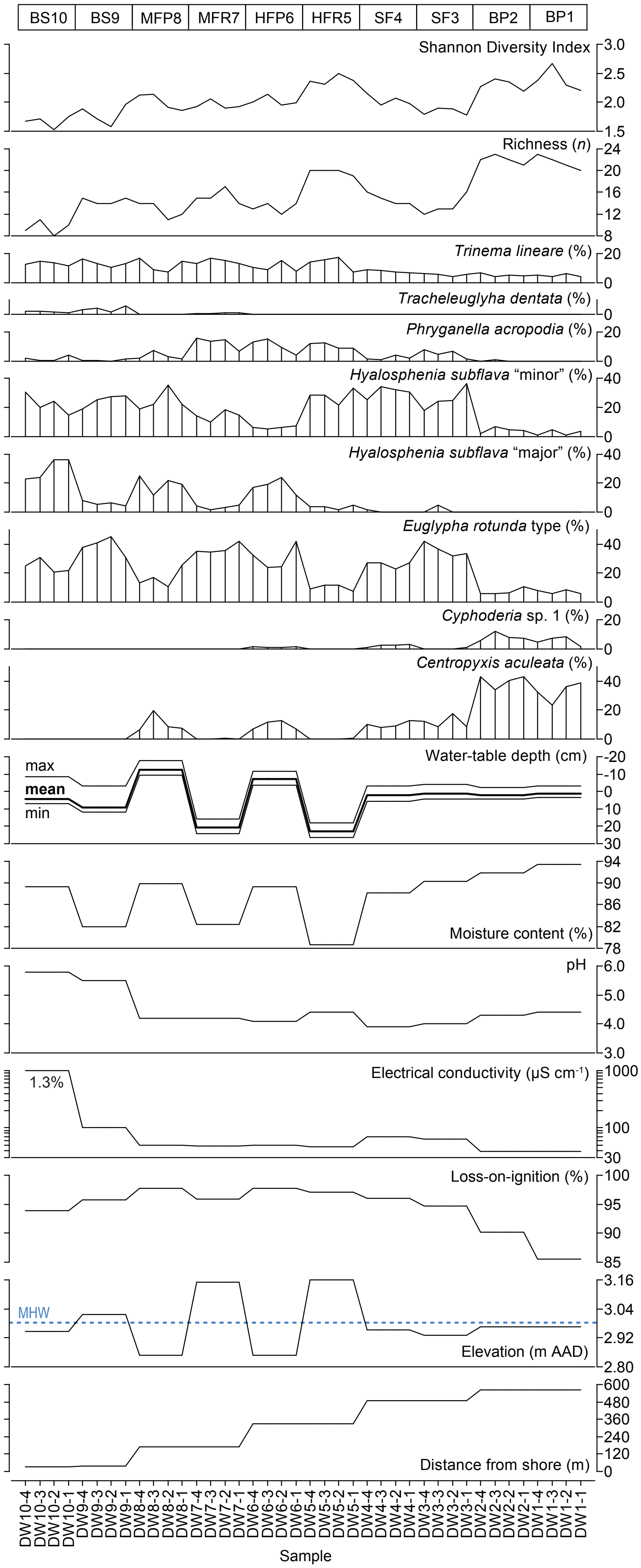

BS10
BS9
MFP8
MFR7
HFP6
HFR5
SF4
SF3
BP2
BP1
Shannon Diversity Index
3.0
2.5
2.0
1.5
Richness (n)
24
20
16
12
8
Trinema lineare (%)
20
0
Tracheleuglyha dentata (%)
0
Phryganella acropodia (%)
20
0
Hyalosphenia subflava "minor" (%)
40
20
0
Hyalosphenia subflava "major" (%)
40
20
0
Euglypha rotunda type (%)
40
20
0
Cyphoderia sp. 1 (%)
20
0
Centropyxis aculeata (%)
40
20
0
Water-table depth (cm)
max
mean
min
-20
-10
0
10
20
30
94
90
86
82
78
Moisture content (%)
pH
6.0
5.0
4.0
3.0
Electrical conductivity (μS cm-1)
1.3%
1000
100
30
Loss-on-ignition (%)
100
95
90
85
MHW
3.16
3.04
2.92
2.80
Elevation (m AAD)
600
480
360
240
120
0
Distance from shore (m)
DW10-4
DW10-3
DW10-2
DW10-1
DW9-4
DW9-3
DW9-2
DW9-1
DW8-4
DW8-3
DW8-2
DW8-1
DW7-4
DW7-3
DW7-2
DW7-1
DW6-4
DW6-3
DW6-2
DW6-1
DW5-4
DW5-3
DW5-2
DW5-1
DW4-4
DW4-3
DW4-2
DW4-1
DW3-4
DW3-3
DW3-2
DW3-1
DW2-4
DW2-3
DW2-2
DW2-1
DW1-4
DW1-3
DW1-2
DW1-1
Sample

Figure 4

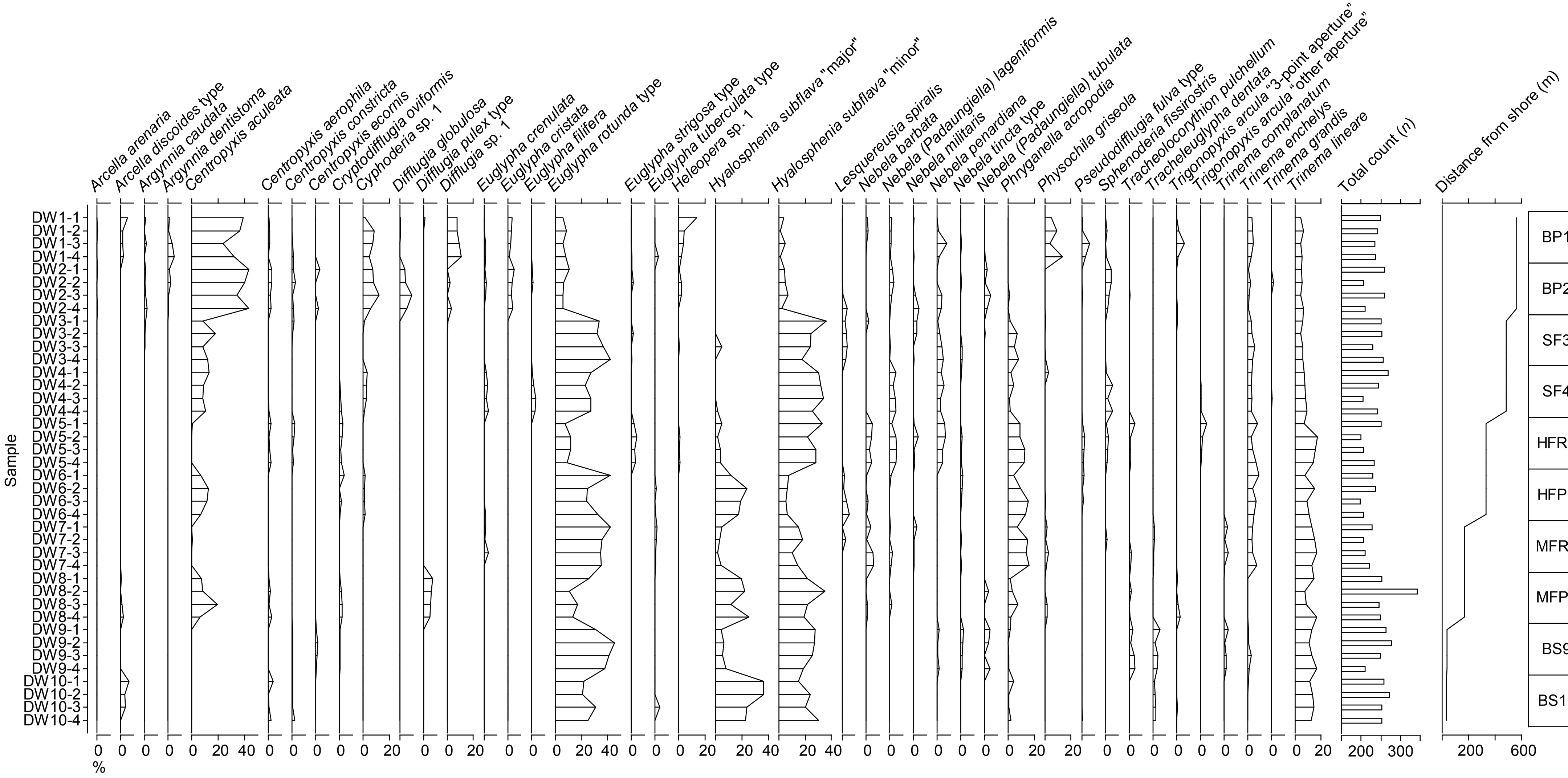
Arcella arenaria
Arcella discoides type
Argynnia caudata
Argynnia dentistoma
Centropyxis aculeata
Centropyxis aerophila
Centropyxis constricta
Centropyxis ecornis
Cryptodifflugia oviformis
Cyphoderia sp. 1
Difflugia globulosa
Difflugia pulex type
Difflugia sp. 1
Euglypha crenulata
Euglypha cristata
Euglypha filifera
Euglypha rotunda type
Euglypha strigosa type
Euglypha tuberculata type
Heleopera sp. 1
Hyalosphenia subflava "major"
Hyalosphenia subflava "minor"
Lesquereusia spiralis
Nebela barbata
Nebela (Padaungiella) lageniformis
Nebela militaris
Nebela penardiana
Nebela tincta type
Nebela (Padaungiella) tubulata
Phryganella acropodia
Physochila griseola
Pseudodifflugia fulva type
Sphenoderia fissirostris
Tracheolocorythion pulchellum
Tracheleuglypha dentata
Trigonopyxis arcula "3-point aperture"
Trigonopyxis arcula "other aperture"
Trinema complanatum
Trinema enchelys
Trinema grandis
Trinema lineare
Total count (n)
Distance from shore (m)
Sample
DW1-1
DW1-2
DW1-3
DW1-4
DW2-1
DW2-2
DW2-3
DW2-4
DW3-1
DW3-2
DW3-3
DW3-4
DW4-1
DW4-2
DW4-3
DW4-4
DW5-1
DW5-2
DW5-3
DW5-4
DW6-1
DW6-2
DW6-3
DW6-4
DW7-1
DW7-2
DW7-3
DW7-4
DW8-1
DW8-2
DW8-3
DW8-4
DW9-1
DW9-2
DW9-3
DW9-4
DW10-1
DW10-2
DW10-3
DW10-4
BP1
BP2
SF3
SF4
HFR5
HFP6
MFR7
MFP8
BS9
BS10
%
0
20
40
200
300
600

Figure 5

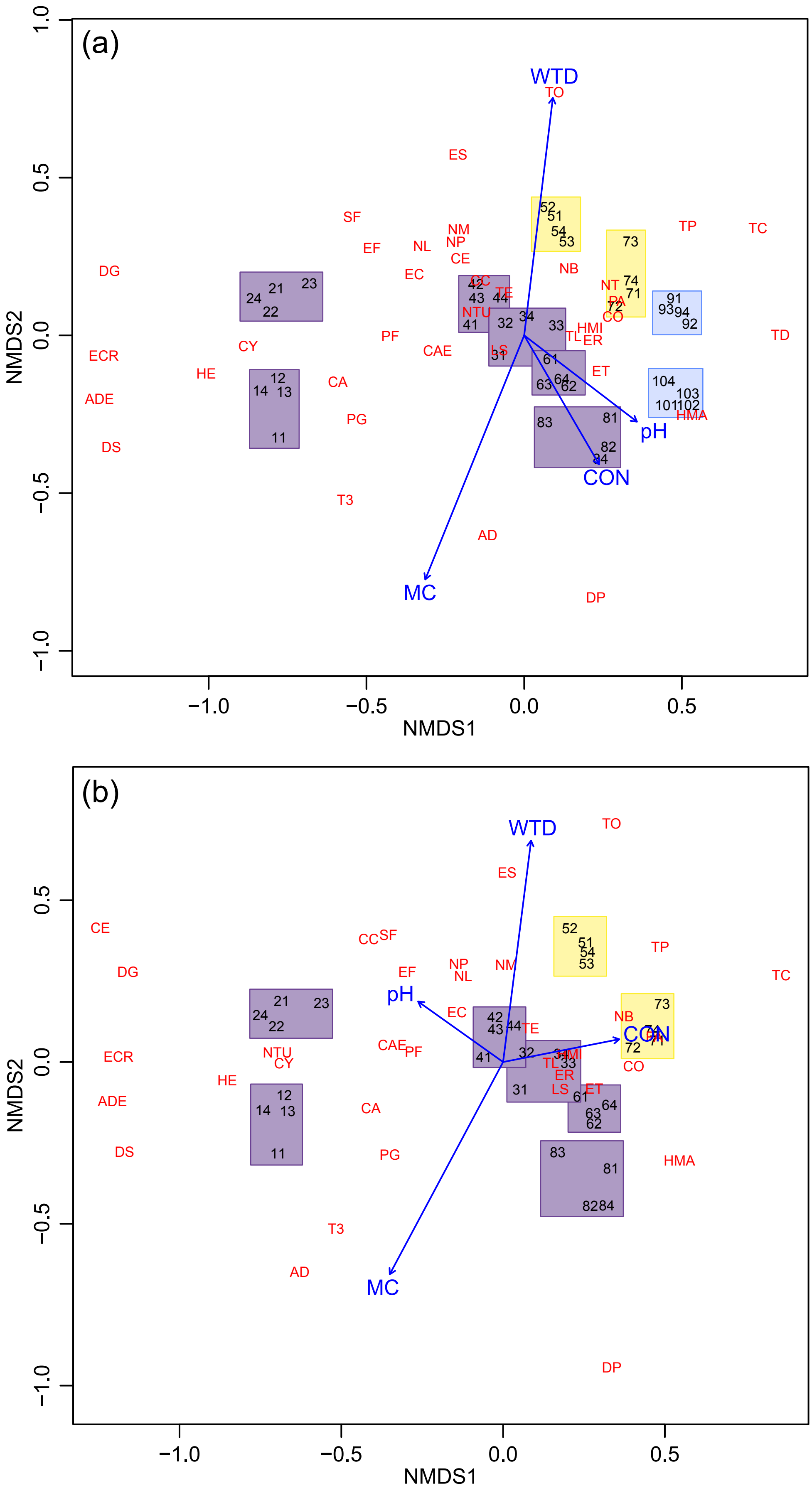
(a)
WTD
pH
CON
MC
NMDS1
NMDS2
−1.0
−0.5
0.0
0.5
1.0
TO
ES
SF
EF
NL
NM
NP
CE
EC
DG
ECR
HE
ADE
DS
CY
CA
PG
PF
CAE
T3
AD
DP
TP
TC
TD
NB
NT
PA
CO
HMI
TL
ER
ET
HMA
LS
NTU
TE
CC
21
22
23
24
11
12
13
14
31
32
33
34
41
42
43
44
51
52
53
54
61
62
63
64
71
72
73
74
81
82
83
84
91
92
93
94
101
102
103
104
(b)
WTD
pH
CON
MC
NMDS1
NMDS2
−1.0
−0.5
0.0
0.5
TO
ES
CE
DG
CC
SF
EF
NP
NL
NM
TP
TC
EC
ECR
NTU
CY
CAE
PF
HE
ADE
DS
CA
PG
T3
AD
DP
HMA
NB
CO
TE
TL
ER
LS
ET
HMI
21
22
23
24
11
12
13
14
31
32
33
34
41
42
43
44
51
52
53
54
61
62
63
64
71
72
73
81
82
83
84

Figure 6

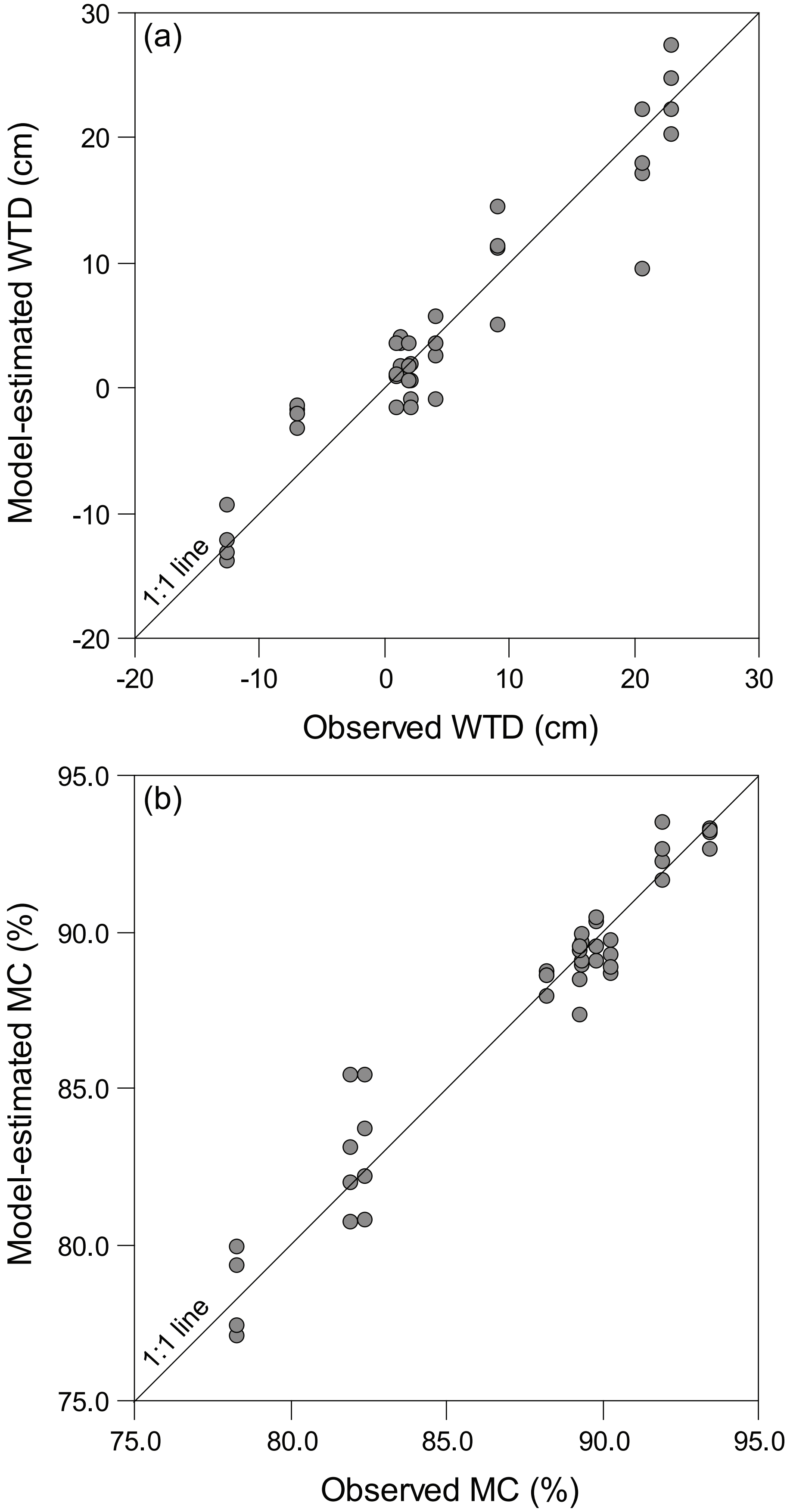

(a)
Model-estimated WTD (cm)
Observed WTD (cm)
1:1 line
30
20
10
0
-10
-20
-20
-10
0
10
20
30
(b)
Model-estimated MC (%)
Observed MC (%)
1:1 line
95.0
90.0
85.0
80.0
75.0
75.0
80.0
85.0
90.0
95.0

Figure 7

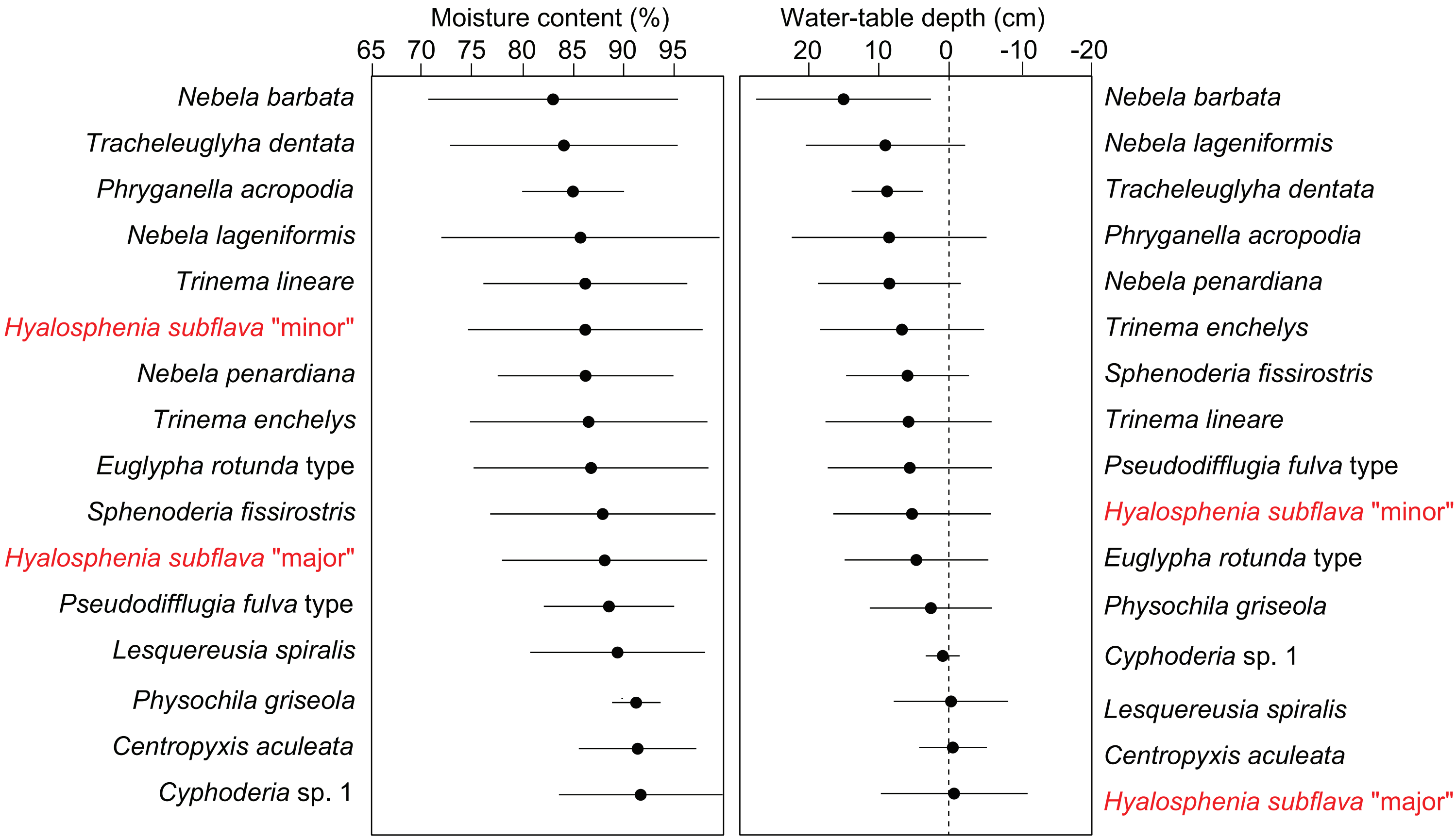

Moisture content (%)
65
70
75
80
85
90
95
Water-table depth (cm)
20
10
0
-10
-20
Nebela barbata
Tracheleuglyha dentata
Phryganella acropodia
Nebela lageniformis
Trinema lineare
Hyalosphenia subflava "minor"
Nebela penardiana
Trinema enchelys
Euglypha rotunda type
Sphenoderia fissirostris
Hyalosphenia subflava "major"
Pseudodifflugia fulva type
Lesquereusia spiralis
Physochila griseola
Centropyxis aculeata
Cyphoderia sp. 1
Nebela barbata
Nebela lageniformis
Tracheleuglyha dentata
Phryganella acropodia
Nebela penardiana
Trinema enchelys
Sphenoderia fissirostris
Trinema lineare
Pseudodifflugia fulva type
Hyalosphenia subflava "minor"
Euglypha rotunda type
Physochila griseola
Cyphoderia sp. 1
Lesquereusia spiralis
Centropyxis aculeata
Hyalosphenia subflava "major"

Figure 8

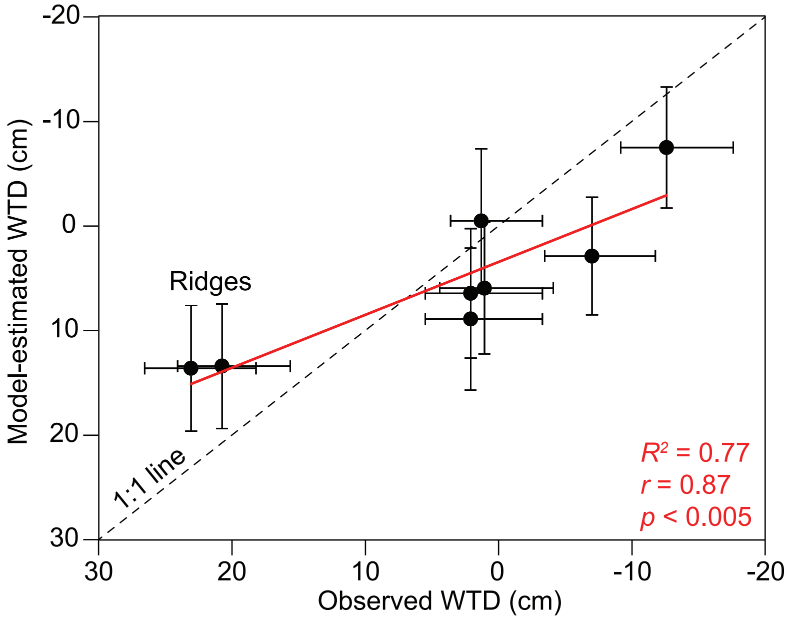

Ridges
1:1 line
R^2 = 0.77
r = 0.87
p < 0.005
Model-estimated WTD (cm)
Observed WTD (cm)
-20
-10
0
10
20
30

Table 1

Dipwell code	Distance from shore (m)	Latitude	Longitude	Vegetation zone	NMDS site code
DW1	565.4	9.38333	-82.36611	Bog plain (BP1)	11-14
DW2	565.4	9.38333	-82.36611	Bog plain (BP2)	21-24
DW3	486.1	9.38278	-82.36556	Stunted forest (SF3)	31-34
DW4	486.1	9.38278	-82.36556	Stunted forest (SF4)	41-44
DW5	330.0	9.38194	-82.36611	Hardwood forest ridge (HFR5)	51-54
DW6	330.0	9.38194	-82.36611	Hardwood forest pool (HFP6)	61-64
DW7	168.6	9.38083	-82.36694	Mixed forest ridge (MFR7)	71-74
DW8	168.6	9.38083	-82.36694	Mxed forest pool (MFP8)	81-84
DW9	37.0	9.37972	-82.36778	Brackish scrub (BS9)	91-94
DW10	31.7	9.37972	-82.36778	Brackish scrub (BS10)	101-104

Table 2

Taxon	Code	Authority
Arcella arenaria	AA	Greeff 1866
Arcella discoides type	AD	Ehrenberg 1843
Argynnia caudata	AC	Leidy 1879
Argynnia dentistoma	ADE	Penard 1890
Centropyxis aculeata	CA	Ehrenberg 1838
Centropyxis aerophila	CAE	Deflandre 1929
Centropyxis constricta	CC	Ehrenberg 1841
Centropyxis ecornis	CE	Ehrenberg 1841
Cryptodifflugia oviformis	CO	Penard 1890
Cyphoderia sp. 1	CY	Schlumberger 1845
Difflugia globulosa	DG	Dujardin 1837; Penard 1902
Difflugia pulex type	DP	Penard 1902
Difflugia sp. 1	DS	Leclerc 1815
Euglypha crenulata	EC	Wailes 1912
Euglypha cristata	ECR	Leidy 1874
Euglypha filifera	EF	Leidy 1874
Euglypha rotunda type	ER	Wailes and Penard 1911
Euglypha strigosa type	ES	Ehrenberg 1872; Leidy 1878
Euglypha tuberculata type	ET	Dujardin 1841
Heleopera sp. 1	HE	Leidy 1879
Hyalosphenia subflava "major"	HMA	Cash and Hopkinson 1909
Hyalosphenia subflava "minor"	HMI	Cash and Hopkinson 1909
Lesquereusia spiralis	LS	Ehrenberg 1840
Nebela militaris	NB	Penard 1890
Nebela barbata	NL	Leidy 1874
Nebela (Padaungiella) lageniformis	NM	Penard 1890
Nebela penardiana	NP	Deflandre 1936
Nebela tincta type	NT	Leidy 1979; Awerintzew 1906
Nebela (Padaungiella) tubulata	NTU	Brown 1911
Phryganella acropodia	PA	Hertwig and Lesser 1874; Cash and Hopkinson 1909
Physochila griseola	PG	Wailes and Penard 1911
Pseudodifflugia fulva type	PF	Archer 1870
Sphenoderia fissirostris	SF	Schlumberger 1845
Tracheolocorythion pulchellum	TP	Penard 1890
Tracheleuglypha dentata	TD	Deflandre 1929
Trigonopyxis arcula "3-point aperture"	T3	Penard 1912
Trigonopyxis arcula "other aperture"	TO	Penard 1912
Trinema complanatum	TC	Penard 1890
Trinema enchelys	TE	Leidy 1878
Trinema grandis	TG	Chardez 1960
Trinema lineare	TL	Penard 1890

Table 3

Water-table depth (cm)	*RMSE*	R^2	*Average bias*	*Maximum bias*	$R^2_{(LOO)}$
WA (inverse deshrinking)	6.60	0.60	2.04E-15	9.44	0.48
WA (classical deshrinking)	8.53	0.60	2.11E-16	8.13	0.51
WA (tolerance downweighted, inverse deshrinking)	4.33	0.83	-2.13E-15	8.57	0.76
WA (tolerance downweighted, classical deshrinking)	4.76	0.83	-1.24E-15	7.98	0.76
WAPLS (component 1)	6.60	0.60	-2.11E-04	9.44	0.48
WAPLS (component 2)	4.89	0.78	6.18E-05	6.11	0.67
WAPLS (component 3)	**3.29**	**0.90**	**9.73E-05**	**4.82**	**0.80**
WAPLS (component 4)	2.97	0.92	4.56E-05	3.78	0.82
WAPLS (component 5)	2.60	0.94	5.04E-05	2.23	0.80
ML	6.51	0.76	-3.74E+00	10.92	0.61
Moisture content (%)	***RMSE***	R^2	***Average bias***	***Maximum bias***	$R^2_{(LOO)}$
WA (inverse deshrinking)	2.77	0.65	1.92E-14	4.98	0.58
WA (classical deshrinking)	3.44	0.65	6.15E-14	5.73	0.59
WA (tolerance downweighted, inverse deshrinking)	2.37	0.74	3.55E-16	6.41	0.68
WA (tolerance downweighted, classical deshrinking)	2.76	0.74	4.26E-15	5.42	0.68
WAPLS (component 1)	2.77	0.65	1.45E-04	4.97	0.58
WAPLS (component 2)	1.66	0.87	1.48E-05	1.94	0.82
WAPLS (component 3)	**1.14**	**0.94**	**-7.94E-06**	**0.69**	**0.89**
WAPLS (component 4)	1.05	0.95	5.60E-06	0.41	0.88
WAPLS (component 5)	0.93	0.96	-9.03E-06	0.47	0.87
ML	3.58	0.46	-9.67E-01	10.90	0.39

Supplementary file 1: Vegetation zones of Oropel Swamp

Zone 1: central sawgrass (*Cladium*)-dominated plain (dipwells 1 and 2)

Zone 2: stunted *Campnosperma panamensis* forest with sawgrass (dipwells 3 and 4)

Zone 3: *Campnosperma panamensis* – *Symphonia globulifera* hardwood forest (dipwells 5 and 6)

Zone 4: mixed *Campnosperma panamensis* – *Euterpe precatoria* – *Raphia taedigera* forest (dipwells 7 and 8)

Zone 5: mangrove edge, brackish *Cassipourea elliptica* and *Chrysobalanus icaco* scrub (dipwells 9 and 10)

Figure S1. Photographs of each of the vegetation zones. Typically the vegetation follows from zone 1 in the dome centre to zone 5 at the dome edge.

The five vegetation zones correspond to the 'phasic communities' identified by *Phillips et al.* [1997], with an increasing canopy height from zones 1 to 3 and then a decrease in height to zone 5. The vegetation in each of the zones is as follows:

Zone 1:
Descriptor: sawgrass (*Cladium*)-dominated plain.
Description: Dominated by *Cladium mariscus* (sawgrass) (species authorities given below) with a few ~10-m-high *Campnosperma panamensis* trees and *Ardisia* sp. shrubs. Some ferns are present at ground level (*Blechnum* sp.). There are also a few scattered *Symphonia globulifera* trees (15–20 m high).
Equivalent to: Cross between phasic communities (PC) 6 and 7 in *Phillips et al.* [1997].

Zone 2:
Descriptor: stunted *Campnosperma* forest with sawgrass.
Description: Short *Campnosperma panamensis* trees (canopy ~15–20 m) with patchy canopy, and shrub layer dominated by *Ardisia* sp. A few *Symphonia globulifera* saplings present. Understory dominated by *Cladium jamaicense* (another species of sawgrass).
Equivalent to: PC6 in *Phillips et al.* [1997].

Zone 3:
Descriptor: *Campnosperma – Symphonia* hardwood forest.
Description: Canopy is ~30 m and quite open (albeit higher than Zone 2). *Campnosperma panamensis* and *Symphonia globulifera* are dominant (*Campnosperma panamensis* is the more common of the two). Understory contains *Euterpe precatoria*, *Tococa guianensis*, *Ouratea sp.* and Myrsinaceae. Also present are *Cassipourea elliptica*, Annonaceae and Mimosoid trees. *Cladium jamaicense* is also found.
Equivalent to: cross between PC4 and 5 in *Phillips et al.* [1997].

Zone 4:
Descriptor: mixed *Campnosperma – Euterpe – Raphia* forest.
Description: Canopy is ~25 m high and composed of *Campnosperma panamensis.* Underneath this there is a thick layer of *Euterpe precatoria* providing a high stem density. There is also some *Raphia taedigera* and *Cassipourea elliptica*.
Equivalent to: cross between PC3 and 4 in *Phillips et al.* [1997].

Zone 5
Descriptor: mangrove-edge *Cassipourea-Chrysobalanus* scrub.
Description: A ~5 m-high canopy dominated by *Cassipourea elliptica* and *Chrysobalanus icaco* shrub. Sawgrass and mangrove fern (*Acrostichum aureum*) in understory. Some Mimosoid trees, *Myrica mexicana* and *Blechnum* sp. fern.
Equivalent to: a subset of PC2 in *Phillips et al.* [1997].

Species authorities:
Acrostichum aureum L.
Campnosperma panamensis Standl.
Cassipourea elliptica Poir.
Chrysobalanus icaco L.
Cladium mariscus (L.) Pohl
Cladium jamaicense Crantz
Euterpe precatoria Mart.
Myrica mexicana Humb. & Bonpl. ex Willd.
Raphia taedigera Mart.
Symphonia globulifera L.f.
Tococa guianensis Aubl.

Supplementary file 1 adapted from:

Baird, A.J., Low, R., Young, D., Swindles, G.T., Lopez, O.R., Page, S., 2017. High permeability explains the vulnerability of the carbon store in drained tropical peatlands. Geophysical Research Letters 44, 1333-1339.